www.czasopisma.pan.pl PAN POLSKA AKADEMIA NAUK www.journals.pan.pl

Arch. Metall. Mater. **68** (2023), 3, 875-880

DOI: https://doi.org/10.24425/amm.2023.145450

A. FAZELI KISOMI[1*], S.J.MOUSAVI[2], B. NEDAEE-SHAKARAB[1]

INVESTIGATION ON STRUCTURAL, ELECTRONIC, THERMAL AND THERMOELECTRIC PROPERTIES OF $Al_{0.25}B_{0.75}As$ ALLOY UNDER PRESSURE, BASED ON DENSITY FUNCTIONAL THEORY (DFT)

In this paper, structural, electronic, thermal, and thermoelectric properties of $Al_{0.25}B_{0.75}As$ alloy, under pressures 0 GPa, 4 GPa and 8 GPa, have been calculated. The value of band gap at present work under 0 GPa, with GGA(PBE) exchange-correlation potential, is very close to other works with TB-mBJ method. This is a result of equal selection of muffin-tin radius spheres that are bigger than usual size for Al and B atoms. The values of band gap decrease by increasing pressure. In thermal properties, phonon contribution of heat capacity at constant volume and Debye temperature have been calculated in the range of 0K to 1000K temperatures and under 0 GPa, 4 GPa and 8 GPa pressures. Thermoelectric properties, under the same pressures and in the range of 100K to 1000K temperatures have been investigated.

Keywords: $Al_{0.25}B_{0.75}As$; Thermoelectric properties; electronic properties under pressure and Wien2k

1. Introduction

The III-V semiconductor ternary alloys, has attracted attention of researchers in recent years [1-5]. They are good candidates for many device applications such as: high-speed electronic and long wave length photonic devices because of their band gaps cover a wide spectral range [6,7]. Among many research conducted on III-V ternary alloys, $Al_{1-x}B_xAs$ alloys have been computationally studied twice, by Boubendira et al. [2] and Moussa et al. [4].

Boron compounds and their semiconductors in electronic and optoelectronic applications areas are extremely attractive for scientists due to their good physical properties including their wide band gap, large resistivity and high thermal conductivity [8-11] as well as low iconicity [12-14].

In the calculation done by Moussa et al. It is confirmed that these alloys are good candidates for optoelectronic usages. Prior to that Boubendira et.al. calculated electronic properties of $Al_{1-x}B_xAs$, including x = 0.75 and other values of x. They plotted the diagram of $Al_{0.25}B_{0.75}As$ heat capacity at constant volume versus temperature in the range of 0K to 500K and under 0 GPa to 8 GPa pressures. However, the electronic and thermoelectric properties of this compound under pressure have not been computationally predicted, up to now. According to our calculations, the values of band gap of this compound decrease by increasing the pressure which leads to improvement of thermoelectric properties. It is important to mention that in our calculations in this study, we obtained the value of band gap close to the results of TB-mBJ method [16] under 0 GPa, by using GGA(PBE) [15] as an exchange-correlation potential. This is because of equal selection of muffin-tin radius spheres for all atoms which are bigger than usual size for Al and B atoms. This can be considered as the novelty of present study.

In the section 2 of this paper, computational details of this research are presented. In result and discussions section (section3), first, we investigate structural properties and then we will discuss electronic properties. In electronic properties, band structures and total DOS diagrams of this compound will be plotted under pressure. Subsequently, thermal properties, consisting of heat capacity at constant volume, and Debye temperature under 0 GPa, 4 GPa and 8 GPa pressures will be investigated. At the end of section 3, the diagrams of thermoelectric properties including Seebeck coefficient, electrical conductivity(divided by relaxation time), power factor, electronic thermal conductivity(divided by relaxation time) and electronic contribution of heat capacity at constant volume in the range of 100K to 1000K temperatures and under the same pressures of thermal properties will be analyzed. Ultimately, (section 4) the results of this research will be concluded.

[1] DEPARTMENT OF PHYSICS, ARDABIL BRANCH, ISLAMIC AZAD UNIVERSITY, ARDABIL, IRAN
[2] DEPARTMENT OF PHYSICS, RASHT BRANCH, ISLAMIC AZAD UNIVERSITY, RASHT, IRAN

* Corresponding author: alif1364@yahoo.com

2. Computational details

Structural and electronic properties have been calculated by computational code Wien2k [17]. E_{cut} = –6 Rydberg, $R_{MT} \times K_{MAX}$ = 7 and number of k-points for super cell 1×1×1 of $Al_{0.25}B_{0.75}As$ 100 have been considered. GGA(PBE) as an exchange-correlation potential has been used. Muffin-tin radius spheres for all 8 atoms equals 1.8 a.u. The equal value for all atoms, which are bigger than usual size for Al and B, leads to increasing band gap in the range of values obtained by TB-mBJ method. Thermal properties have been obtained by code GIBBS2 [18,19], using energy-volume data from output files of Wien2k code. We use Debye-Gruneisen method for these calculations. Thermoelectric properties have been calculated by accessorial code BoltzTrap [20], by using output files of Wien2k code consisting of case.struct and case.energy.

3. Results and Discussions

3.1. Structural Properties

Present structure is zinc-blende super cell 1×1×1 of AlAs with 8 basic atoms, in which 3 atoms B were replaced with 3 atoms Al and one atom of Al remained unchanged. The diagram of energy-volume data was fitted with Murnaghan EOS. The diagram (Fig. 1) has a parabolic shape which indicates the stability of the compound.

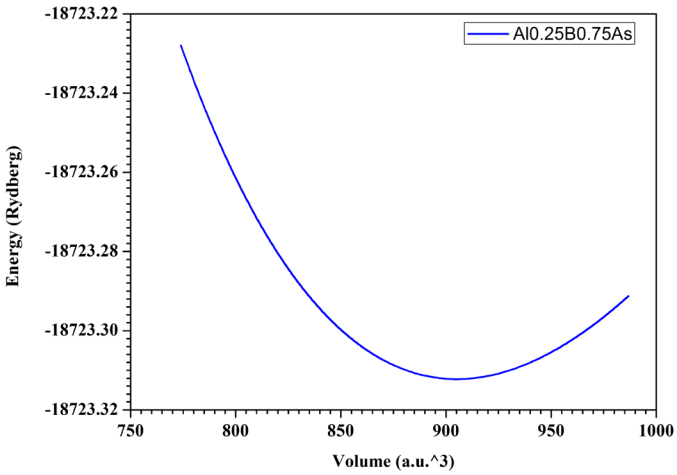

Fig. 1. The diagram of energy-volume data for super cell 1×1×1 of $Al_{0.25}B_{0.75}As$ alloy

Structural properties obtained for $Al_{0.25}B_{0.75}As$ alloy in this research have been compared to other theoretical studies for this compound and experimental work for BAs in TABLE 1.

As can be seen lattice constant in comparison with BAs has an increment that is due to presence of Al atom and its bigger radius compare to B atom. In addition, Bulk modulus of BAs is larger than $Al_{0.25}B_{0.75}As$. This is due to smaller covalent radius of B than Al as well as stronger binding of B-As than Al-As. Hence,

TABLE 1

Structural properties of $Al_{0.25}B_{0.75}As$ under 0 GPa, 4 GPa and 8 GPa pressures and comparison them with other works under 0 GPa

	Our work 0 GPa	Our work 4 GPa	Our work 8 GPa	Other calculations	BAs (experimental)
a (A°)	5.1188	5.0530	4.9988	5.07 [2] and 5.113 [4]	4.77[21]
B (GPa)	97.5017	—	—	110.41 [2] and 99.86 [4]	173[21]
B'	4.3847	—	—	4.095 [4]	—

BAs demonstrates more resistance against pressure and is harder than $Al_{0.25}B_{0.75}As$. Furthermore, in TABLE 1, lattice constant of $Al_{0.25}B_{0.75}As$ under 4 GPa and 8 GPa pressures have been listed although in absence of other experimental or theoretical work, comparison is impossible. Under 0 GPa our study has a good agreement under 0 GPa, especially with another GGA(PBE) work [4] that supports validity of our calculations.

3.2. Electronic properties

3.2.a). Band structures under 0 GPa, 4 GPa and 8 GPa Pressures

In Figs. 2a to c, The diagrams of band structures for $Al_{0.25}B_{0.75}As$ under pressures 0 GPa, 4 GPa and 8 GPa have been plotted. The values of band gap obtained in present study, under those pressures, have been compared to other theoretical researches on $Al_{0.25}B_{0.75}As$ and an experimental study on BAs under 0 GPa in TABLE 2. Our research demonstrates a good growth in value of band gap in comparison with other GGA(PBE) work and has a good consistency with other TB-mBJ works for $Al_{0.25}B_{0.75}As$ under 0 GPa. This is due to increase in band gap, as a result of an equal selection value for muffin-tin radius spheres ,which are bigger than usual size for Al and B atoms that lead to increasing coulomb interaction among atoms. When coulomb interaction increases, band gap increases, too [22].

TABLE 2

The values of band gap in present work for $Al_{0.25}B_{0.75}As$ under 0 GPa, 4 GPa, 8 GPa pressures and comparison them with other works under 0 GPa

Our work 0 GPa	Our work 4 GPa	Our work 8 GPa	Other calculations	BAs (experimental)
1.64	**1.58**	**1.57**	**1.573 (TB-mBJ) [2] and 1.681 (TB-mBJ) [4] 1.191 (GGA-PBE) [4]**	**1.45 [21]**

By increasing pressure, the slope of bands in band structures in most of energies decreases resulting an increasing effective mass. The trace of this fact is visible in thermoelectric properties.

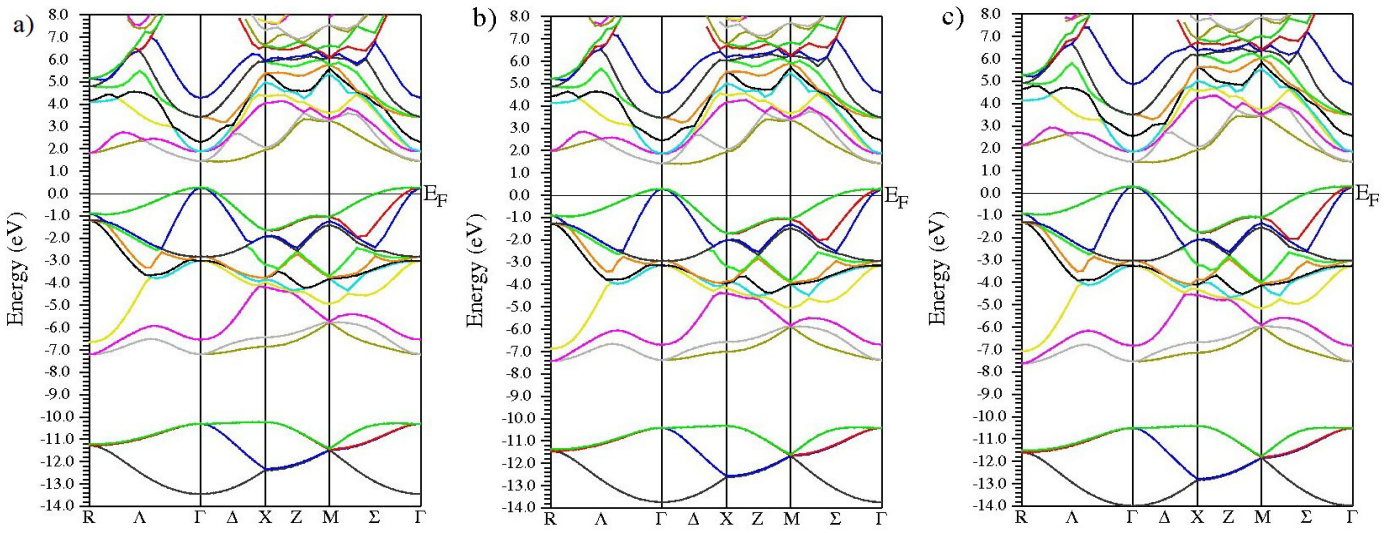

Fig. 2. The diagrams of band structures for $Al_{0.25}B_{0.75}As$ alloy under pressures a) 0 GPa, b) 4 GPa and c) 8 GPa

Band gap of this compound decreases by increase in hydrostatic pressure. This is because semiconductors are quantum in nature. Hydrostatic pressure acts like a perturbation on periodic potential and breaks the cubic symmetry of cubic structure and moves down the nearest bands in conduction band which are degenerate. While, this reduction in values of band gap, in the range of 0 GPa to 4 GPa, is 0.07ev, the result in the range of 4 GPa to 8 GPa is only 0.01ev. This is due to increasing coulomb interaction among atoms which lead to a decreasing the reduction in band gap.

The value of band gap in BAs is less than $Al_{0.25}B_{0.75}As$. This is because Al is heavier than B leading to increasing coulomb interaction and resulting a larger band gap. Band gap of $Al_{0.25}B_{0.75}As$ as obtained in present work is direct band gap at Γ point, whereas band gap of BAs is indirect band gap (Γ-X).

It is noticeable that present work for band structure diagram under 0 GPa has a good consistency with other TB-mBJ studies [2,4].

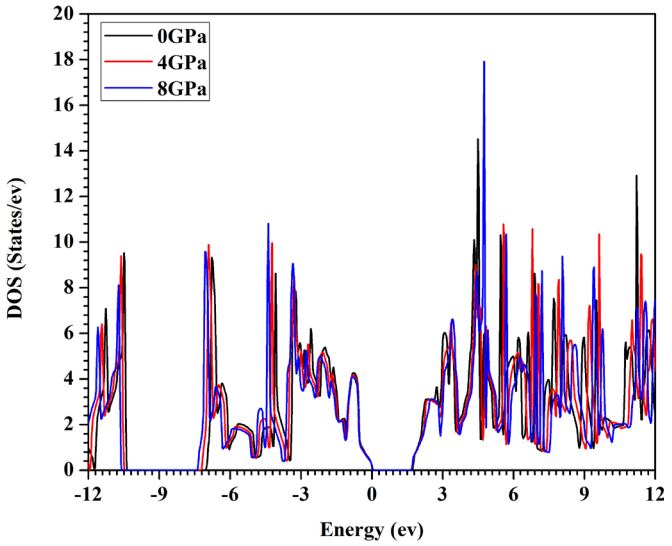

Fig. 3. The diagram of total Density Of States for $Al_{0.25}B_{0.75}As$alloy under 0 GPa, 4 GPa and 8 GPa pressures

3.2.b). Total Density Of States under 0 GPa, 4 GPa and 8 GPa Pressures

As demonstrated in Fig. 3 in total Density of States diagram, apart from reduction in band gap peaks move to more negative energies in valence band, while they move to more positive energies in conduction band. These are due to abandon equilibrium and decrease in stability, although in a few points some changes in intensity and places of peaks have been occurred. As mentioned, flatness of bands in band structure in most of energies increases By increasing pressure. By considering this note that the sharpest peak belongs to 8 GPa in conduction band, this subject has been confirmed.

Van Hove singularities are the sharp peaks of DOS diagram. When $\nabla_k \varepsilon = 0$, the sharp peaks appear in DOS diagram that indicates the bands in band structure are flat or denser in that energy. The biggest Van Hove singularity belongs to 8 GPa near the 4ev.

3.3. Thermal properties

As demonstrated in Figs. 4a and b thermal properties consisting of phonon contribution of heat capacity at constant volume and Debye temperature for $Al_{0.25}B_{0.75}As$ alloy in the range of 0K to 1000K and under 0 GPa, 4 GPa and 8 GPa pressures have been calculated. Heat capacity at constant volume under all of the pressures at low temperatures has T^3 Debye behavior and at high temperatures trends to saturation Dulong-Petit limit. The reason of increase in heat capacity by increasing temperature is rise in phonon oscillations affected by increment in temperature. In the next section we will discuss about electronic contribution of heat capacity at constant volume. By increasing pressure phonon contribution of heat capacity at constant volume decreases. This is due to reduce in volume and restriction of possibility of atoms oscillations affected by pressure increasing that itself is a result of increment in coulomb interaction among atoms.

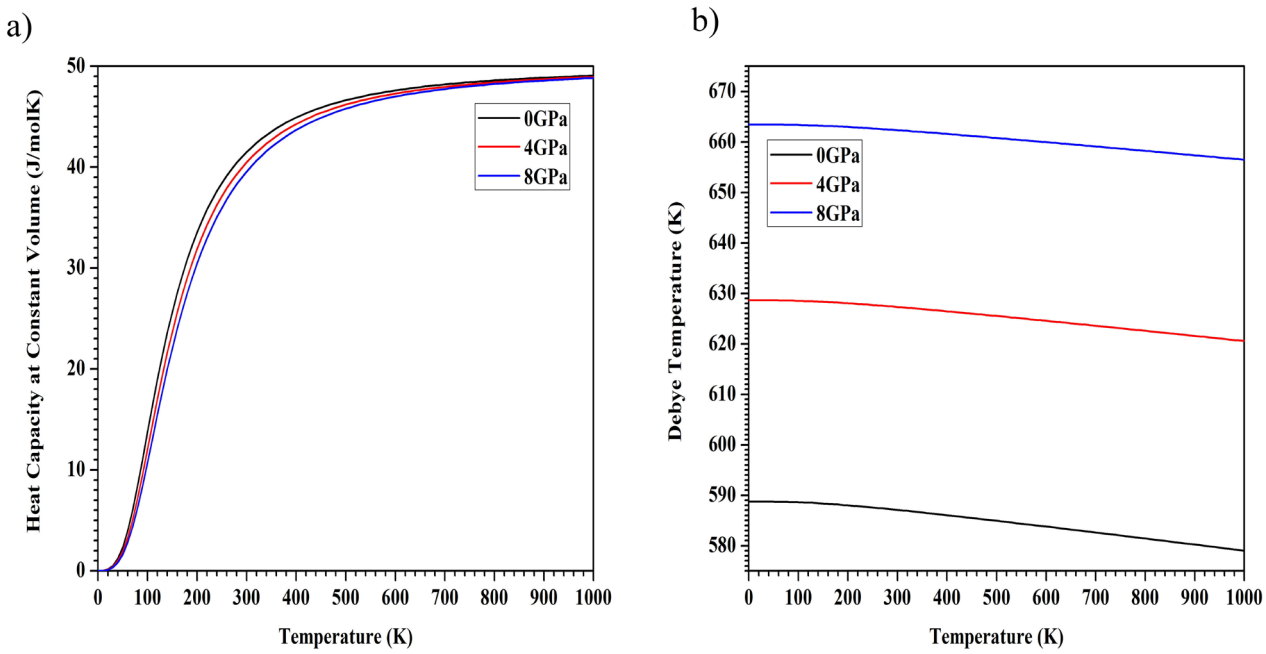

Fig. 4. Thermal properties of $Al_{0.25}B_{0.75}As$ alloy versus temperature in the range of 0K to 1000K temperatures under 0 GPa, 4 GPa and 8 GPa pressures a) Phonon contribution of heat capacity at constant volume, b) Debye temperature

In Fig. 4b Debye temperature slowly decreases by increasing temperature which lead to increase in atoms oscillations and subsequent increase in sound scattering and reduction in sound velocity. This is due to direct relation between Debye temperature and sound velocity. by increasing pressure and reducing volume, Debye temperature increases. This is due to invert relation between Debye temperature and volume. By reducing in volume, atoms oscillations decrease due to increasing coulomb interaction. This lead to increasing sound velocity in alloy.

3.4. Thermoelectric properties

In Figs. 5a to e thermoelectric properties of $Al_{0.25}B_{0.75}As$ alloy versus temperature in the range of 100K to 1000K temperatures under 0 GPa, 4 GPa and 8 GPa pressures have been plotted. In Fig. 5a the diagrams of Seebeck coefficient versus temperature have been demonstrated. Under different pressures, and by increasing temperature to 450K, the diagrams have a descending behavior, followed by a climb to 800K. These diagrams' trend in final 200K reach to saturation limit. From 100K to 450K charge carriers are electrons and these electrons arrive at the end of solid body and produce an electric field opposite of temperature gradient. When the ascending behavior of diagrams starts i.e. affected by heat, electrons are excited to conduction band and charge carriers convert to holes. When enough electrons are excited, Seebeck coefficient tends to saturation limit. Increase in flatness of band structure by increasing pressure, increases Seebeck coefficient by enhanced effective mass. Moreover, when volume decreases, electrons arrive at the end of solid body faster. By increasing pressure, value of band gap decreases and small band gap can improve Seebeck coefficient.

The diagrams of electrical conductivity divided by relaxation time under different pressures have been demonstrated in Fig. 5b. Since the number of excited electrons to conduction band affected by heat, exponentially changes with 1/T, the diagram of electrical conductivity in semiconductors must be ascending. According to our calculations, in most temperatures under different pressures, it confirmed the correction of our calculations. Also, as mentioned, by increasing pressure in this compound effective mass increases. This note appears at low temperatures in electrical conductivity under different pressure. So that, at 100K electrical conductivity under 0 GPa is more than that of under 8 GPa and 4 GPa, while in above 300K by increasing pressure electrical conductivity increases. This is due to reduction in volume and faster traveling electrons in solid body.

Power factor with formula $(S^2\sigma)/\tau$ whose high value indicates the compound is a good thermoelectric material. In Fig. 5c under different pressures versus temperature has been plotted. Because of increasing Seebeck coefficient by increasing pressure and that electrical conductivity in most temperatures (above 300K) has the same behavior, Power factor increases by increasing pressure. However, power factor by increasing temperature has the same behavior of Seebeck coefficient i.e. first it has a descending behavior and then has an ascending trend. However, because of increase in electrical conductivity at high temperatures power factor has not tend to saturation limit.

In Fig. 5d, the diagrams of electronic thermal conductivity divided by relaxation time versus temperature, under 0 GPa, 4 GPa and 8 GPa pressures, have been demonstrated. Electronic thermal conductivity increases by increment in temperature because of faster moving of electrons in solid body. According to Wiedmann-Franz law, electronic thermal conductivity has a direct relation to electrical conductivity and temperature and

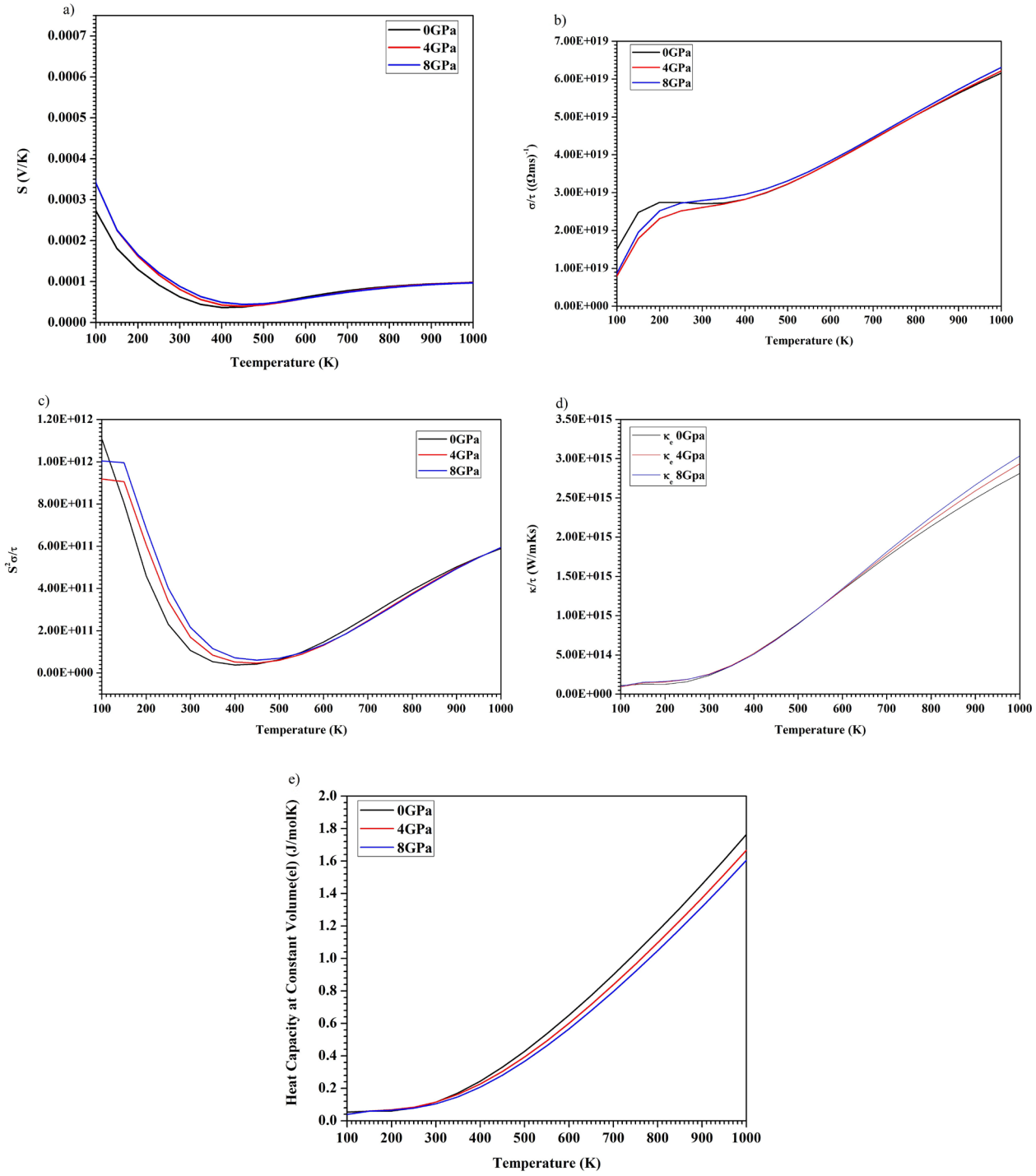

Fig. 5. Thermoelectric properties of $Al_{0.25}B_{0.75}As$ alloy versus temperature in the range of 100K to 1000K temperatures under 0 GPa, 4 GPa and 8 GPa pressures a) Seebeck coefficient, b) electrical conductivity divided by relaxation time, c) power factor, d) electronic thermal conductivity divided by relaxation time, e) electronic contribution of heat capacity at constant volume

Both increase by increasing temperature. by increasing pressure because of reduction in volume, electrons move faster in solid body and electronic thermal conductivity increases.

In Fig. 5e, the diagrams of electronic contribution of heat capacity versus temperature in the range of 100K to 1000K temperatures, under 0 GPa, 4 GPa and 8 GPa pressures, have been plotted. By increasing temperature because of increment in electrons oscillations, electronic contribution of C_V increases, while by increasing pressure and decreasing in volume, electron oscillations are restricted because of increasing coulomb interaction. Therefore, electronic contribution of C_V decreases.

As shown in Figs. 5a to c electrical conductivity divided by relaxation time is in the range of 10^{19} which is noticeable since this alloy is semiconductor. The Seebeck coefficient is in the range of 10^{-4} to 10^{-5} V/K that except at very low temperatures is not considerable. Power factor at very low temperatures is close to 10^{12} and at very high temperatures is near the 6×10^{11}. At low temperatures because of better Seebeck coefficient at low

temperature in comparison with higher temperatures. The value at high temperatures, because of increase in electrical conductivity, are better than middle temperatures.

4. Conclusion

In this paper, structural, electronic, thermal and thermoelectric properties of $Al_{0.25}B_{0.75}As$ alloy under pressures 0 GPa, 4 GPa and 8 GPa have been investigated. Structural properties have a good agreement with other works. Lattice constant under 0 GPa pressure in comparison with BAs under this pressure has an increment. This is due to bigger atomic radius of Al than B Bulk modulus of $Al_{0.25}B_{0.75}As$. It is due to smaller covalent radius of B than Al and stronger bindings in BAs than $Al_{0.25}B_{0.75}As$. In electronic properties, band gap at 0 GPa, 1.64ev was obtained by GGA(PBE) potential that is close to values obtained by TB-mBJ method and is larger than another GGA(PBE) work. The reason is equal selection of muffin-tin radius spheres that is bigger than usual size for Al and B. By increasing pressure band gap decreases. In thermal properties, phonon contribution of heat capacity at constant volume by increasing temperature at low temperatures under all pressures has T^3 Debye behavior and at high temperatures trends to Dulong-Petit limit. Debye temperature gradually decreases by increasing temperature and increases by increase in pressure. In thermoelectric properties, electrical conductivity divided by relaxation time is in the range of 10^{19}, and considering that this compound is semiconductor, it is noticeable. Power factor at low temperatures is in the range of 10^{12} and at very high temperatures is in the range of 6×10^{11}. Furthermore, Seebeck coefficient, electronic thermal conductivity divided by relaxation time and electronic contribution of heat capacity at constant volume versus temperature under 0 GPa, 4 GPa and 8 GPa pressures have been calculated.

REFERENCES

[1] F. El Haj Hassan, A. Breidi, S. Ghemid, B. Amrani, H. Meradji, O. Pagès, J. Alloys Compd. **499**, 80-89 (2010).

[2] K. Boubendira, H. Meradji, S. Ghemid, F.H. Hassan, Mater. Sci. Semicond. Process **16**, 2063-2069 (2013).

[3] A. Fazeli Kisomi, S.J. Mousavi, Pramana. J. Phys. **91**, 18 (2018).

[4] R. Moussaa, A. Abdiche, R. Khenatab, S.B. Omran, Mater. Res. Express. **6**, 105902 (2019).

[5] K. Boubendira, S. Bendaif, O. Nemiri, A. Boumaza, H. Meradji, S. Ghemid, F. El Haj Hassan, Chin. J. Phys. **55**,1092-1102 (2017).

[6] K. Iga, S. Kinoshita, Process Technology for Semiconductor Lasers, Springer-Verlag, Berlin, (1996).

[7] M. Quillec, Materials for Optoelectronics, Kluwer Academic Publ., Boston (1996).

[8] O.A. Golikova, Phys. Status Solidi A**51**, 11-40 (1979).

[9] N. Chimot, J. Even, H. Folliot, S. Loualiche, Physica B. **364**, 263-272 (2005).

[10] M. Ferhat, A. Zaoui, M. Certier, H. Aourag, Physica B. **252**, 229-236 (1998).

[11] B. Bouhafs, H. Aourag, M. Ferhat, M. Certier, J. Phys. Condens. Matter. **11**, 5781 (1999).

[12] A. Zaoui, F. El Haj Hassan, J. Phys. Condens. Matter. **13**, 253 (2001).

[13] R.M. Wentzcovich, K.J. Chang, M.L. Cohen, Phys. Rev. B. **34**, 1071 (1986).

[14] A. Garcia, M.L. Cohen, Phys. Rev. B. **47**, 4215 (1993).

[15] J. Perdew, K.P. Burke, M. Ernzerhoff, Phys. Rev. Lett. **77**, 3865-3868 (1996).

[16] F. Tran, P. Blaha, Phys. Rev. Lett. **102**, 226401 (2009).

[17] P. Blaha, G.K.H. Madsen, D. Kvasnicka, J. Luitz, WIEN2K, an Augmented Plane Wave Plus Local OrbitalsProgram for Calculating Crystal Properties (Vienna, Austria, 2008).

[18] A. Otero-de-la-Roza, V. Luaña, Comput. Phys. Commun. **182**, 1708-1720 (2011).

[19] A. Otero-de-la-Roza, D. Abbasi-Pérez, V. Luaña, Comput. Phys. Commun. **182**, 2232-2248 (2011).

[20] G.K.H. Madsen, D.J. Singh, Comput. Phys. Commun. **175**, 67-71 (2006).

[21] S. Adachi, "Properties of group-IV, III-V and II-VI semiconductors." Wiley Series in Materials for Electronic and Optoelectronic Applications, edited by P. Capper, S. Kasap, and A. Willoughby, England Wiley, (2005).

[22] A. Anjami, A. Boochani, S.M. Elahi, H. Akbari, Results Phys. **7**, 3522-3529 (2017).